Pulse oximetry: theoretical and experimental models

J. P. de Kock L. Tarassenko

Medical Engineering Unit, Department of Engineering Science, Oxford University, Oxford OX1 3PJ, UK

Abstract—*In the paper a pulse oximetry model is developed using an approach which combines both theoretical and empirical modelling. The optical properties of whole blood are measured as a function of cuvette depth by transmission spectrophotometry using red (660 nm) and infra-red (950 nm) light-emitting diodes as light sources. Twersky's theoretical model gives the best fit to the experimental data. A simple theoretical model which takes into account the nonlinear relationship between optical density and cuvette depth is then used to obtain an expression for the R:IR ratio, which relates the measurement of transmission at the two wavelengths. The R:IR ratio is found to be more or less independent of cuvette depth (SD = 0·14 at 100 per cent SaO_2). To validate the predictions of the theoretical model, the results of a previous experiment in which the relationship between SaO_2 and the R:IR ratio was recorded using a flexible cuvette are used. The experimental values are found to lie within one standard deviation from the theoretical curve relating SaO_2 and the R:IR ratio. It is argued that a reasonably accurate model for pulse oximetry which is based on whole blood and not haemoglobin solutions has been developed.*

Keywords—*Experimental models, In vitro model, Pulse oximetry, Theoretical model*

Med. & Biol. Eng. & Comput., 1993, **31**, 291–300

1 Introduction

THE PULSE OXIMETER is a noninvasive optical instrument which measures arterial oxygen saturation (SaO_2) in a pulsatile vascular bed such as the fingertip or earlobe. SaO_2 is defined as:

$$SaO_2 = \frac{C_o}{C_o + C_r} \times 100 \text{ per cent} \quad (1)$$

where C_o and C_r are the concentrations of oxyhaemoglobin HbO_2, and reduced haemoglobin (or deoxyhaemoglobin) Hb, in the blood sample. Pulse oximetry relies on the difference in absorption spectra between HbO_2 and Hb. Dual-wavelength measurements are usually made by placing a probe containing two light-emitting diodes (LEDs) whose spectral peaks are in the red and infra-red regions, and a photodiode on opposite sides of the vascular bed. The photodiode senses the light transmitted through the tissues, which comprises an alternating (AC) signal due to absorption by pulsatile arterial blood superimposed on a steady-state (DC) level arising from attenuation by venous blood, skin pigments and other nonpulsatile components. With most instruments, the DC level at each wavelength is used to normalise the corresponding AC signal amplitude. The ratio of these AC amplitudes at the two wavelengths has been shown to be a function of the arterial oxygen saturation, and this is the basis of the technique of pulse oximetry (WUKITSCH *et al.*, 1988).

The first pulse oximeters were developed in Japan during the late 1970s. In this early work, whole blood was considered simply to be made up of Hb and HbO_2 solutions which obeyed the Beer-Lambert Law (YOSHIYA *et al.*, 1980). This law describes the absorption of monochromatic light in the nonscattering solution:

$$I = I_0 10^{-\varepsilon CD} \quad (2)$$

where I_0 and I are the incident and transmitted light intensities through a cuvette of depth D, containing a solution of concentration C and with an extinction coefficient ε. Eqn. 2 may be rewritten in terms of optical density OD as:

$$OD = \log\left(\frac{I_0}{I}\right) = \varepsilon CD \quad (3)$$

Experience soon showed, however, that such a simple model gave a poor correlation between pulse oximeter readings and invasive measurements of arterial oxygen saturation (SHIMADA *et al.*, 1984). For instance, at 80 per cent SaO_2 the pulse oximeter overestimated the saturation by approximately 5 per cent, an error which is clinically unacceptable.

As recognised by these early workers (SHIMADA *et al.*, 1984), this discrepancy is due to light scattering phenomena. KRAMER *et al.* (1951), ANDERSON and SEKELJ (1967) and others had already conclusively shown that the Beer-Lambert law is not valid for whole blood, for which the optical density is nonlinear with respect to cuvette depth and haematocrit. In addition KRAMER *et al.* (1951) also reported that the optical density of whole blood is approximately 7–20 times greater than that of haemoglobin solutions. In whole blood, light scattering arises from the discontinuity in refractive index at the plasma/red blood

First received 25th March and in final form 30th September 1991

cell interface, the wavelength of light in the red and infra-red being of the same order of magnitude as the dimensions of a red blood cell. The high concentration of red blood cells in whole blood ensures that light scattered once is likely to be scattered again—hence the phenomenon of multiple scattering.

The complex optical properties of whole blood are such that, in practice, all commercial pulse oximeters are now empirically calibrated using procedures in which hypoxia is induced in normal subjects (SEVERINGHAUS and NAIFEH, 1987). As soon as steady-state hypoxia is reached, the values of the normalised red:infra-red ratio, and of SaO_2, as measured from an arterial blood sample, are recorded. If such data are collected from a large number of volunteers, over a range of oxygen saturations, an empirical calibration curve can be obtained. The majority of such tests are carried out when the SaO_2 is greater than 70 per cent, the lowest tolerable steady-state hypoxia. Below this saturation, the calibration curve is largely estimated by extrapolation.

In an attempt to develop a model relating SpO_2* and dual-wavelength measurements on whole blood, we adopted a similar approach to that of STEINKE and SHEPHERD (1986). To study the relative importance of scattering and absorption, they measured the optical density of whole blood as a function of haematocrit and also the optical density of haemolysed blood as a function of haemoglobin concentration. They then fitted a number of mathematical models for the optical properties of whole blood to their experimental data and found Twersky's multiple scattering theory (TWERSKY, 1962; 1970*a*; *b*) to be the most appropriate. With the use of Twersky's theory they investigated the role of light scattering in whole blood oximetry and concluded that scattering effects did not affect the linearity of whole blood oximeters. Instead, scattering effects were said to increase the sensitivity of these oximeters by contributing linearly to the total optical density change that occurs with altered oxygenation (STEINKE and SHEPHERD, 1986).

To extend this approach to pulse oximetry, we measured the optical density of whole and also of haemolysed blood as a function of cuvette depth. We chose the latter variable rather than haematocrit in view of the fact that pulse oximeters rely on arterial volume pulsations which are essentially changes in optical pathlength. We fitted three different theoretical models of optical transmission in whole blood to our experimental data to determine which model might be the most applicable for the pulsatile case. The model which gave us the closest fit was then used to obtain a relationship between SaO_2 and our dual-wavelength measurements.

1.1 *Optical theories of whole blood*

Among the many theories proposed to study the optical properties of whole blood, three have found general acceptance: Zdrojkowsi and Pisharoty's approach based on photon diffusion theory, Twersky's analytical multiple scattering theory, and the Kubelka-Munk theory. All three approaches are now reviewed in the context of their applicability to pulse oximetry.

1.2 *Photon diffusion theory*

Photon diffusion theory, also known as radiative transfer theory, is based on observations of the transport characteristics of wave intensities. It relies on a differential equation called the equation of transfer which is equivalent to the Boltzmann equation used in the kinetic theory of gases (ISHIMARU, 1978; JOHNSON, 1970). ZDROJKOWSKI and PISHAROTY (1970) solved the diffusion equation for a collimated light beam incident on a slab of blood incorporating the concept of mean optical pathlength of photons in dense scattering media previously derived by SHOCKLEY (1962). Zdrojkowski and Pisharoty derived the following optical density equation of whole blood:

$$OD = -\log\left[e^{-Bd} + \frac{Q}{S(B^2 - Q^2)\sinh(Qd)} \times \left\{1 - e^{-Bd}\left(\cosh(Qd) + \frac{B}{Q}\sinh(Qd)\right)\right\}\right] \quad (4)$$

where

$$B = \frac{1}{L} + \frac{1}{S} \quad (5)$$

$$Q = \frac{3}{2}\sqrt{\frac{B}{L}} \quad (6)$$

$$S = \frac{S_0(\lambda)}{H(H-1)} \quad (7)$$

$$L = \frac{\log(e)}{\varepsilon C_{Hb}} \times 1{\cdot}64 \quad (8)$$

and L is the mean optical path travelled by a photon before absorption, S is the mean optical path before scattering, ε is the extinction coefficient in litre mmol^{-1} cm^{-1}, C_{Hb} is the concentration of haemoglobin in the whole blood sample in g dl^{-1}, H the fractional haematocrit and d the cuvette depth.

1.3 *Twersky's analytical multiple scattering theory*

Twersky's analytical multiple scattering theory of light by large low-refracting and absorbing particles is based on electromagnetic wave theory (TWERSKY, 1962; 1970*a*; *b*). Twersky started by first considering the scattering and absorption effects of a single particle, and then introduced the interaction of many particles and statistical averages to finally arrive at an analytical solution to the multiple scattering problem. ANDERSON and SEKELJ (1967), LIPOWSKY *et al.* (1980) and STEINKE and SHEPHERD (1986) have shown this theory to be applicable to whole blood. Twersky's equation for the variation of optical density is as follows:

$$OD = \log\left(\frac{I_0}{I}\right) = \varepsilon CD - \log_{10}\left[(1-q)10^{-\beta} + q10^{-\delta}\right] \quad (9)$$

where

$$\beta = aDH(1-H) \quad (10)$$

$$\delta = \frac{2q'maDH(1-H)}{2m + aD(1-H)} \quad (11)$$

$$m = \frac{\varepsilon CD}{H} \quad (12)$$

and

a = constant depending on particle size, wavelength, photodiode aperture and refractive indices of plasma and red blood cells

**Notation based on recommendation by PAYNE and SEVERINGHAUS (1986). Pulse oximeter readings are denoted by SpO_2 and direct in vitro measurements from arterial blood samples are denoted by SaO_2.*

q = constant depending on particle size, wavelength and refractive indices
q' = constant depending on the optical arrangement.

The above equation may be interpreted as follows: the εCD term is that given by the Beer-Lambert Law; it represents absorption OD_{abs} and is linear with respect to haematocrit. The second term is a measure of the coherent and incoherent scattering OD_{scat}. It is a parabolic function of H and is symmetric about $H = 0{\cdot}5$. One of the most interesting features of this model is that the total optical density OD_{tot} can be resolved into two distinct and independent parts; thus $OD_{tot} = OD_{scat} + OD_{abs}$ (STEINKE and SHEPHERD, 1986).

1.4 *Two-flux Kubelka-Munk theory*

The Kubelka-Munk theory is a phenomenological approach based on two light fluxes travelling in opposite directions in a homogeneous slab of material which exhibits scattering and absorption effects (KUBELKA and MUNK, 1931; JANSSEN, 1972; ISHIMARU, 1978). This theory assumes diffuse monochromatic illumination of the sample, random distribution of particles whose size is small compared with the sample thickness, negligible specular reflection, and finally isotropic scattering in the medium. These assumptions allow two coupled differential equations to be derived. The solution leads to the following results:

$$OD = \frac{(1 - \theta)e^{-\alpha d}}{1 - \theta e^{-2\alpha d}} \tag{13}$$

where

$$\alpha = \sqrt{K^2 + 2KS} \tag{14}$$

$$\theta = \frac{S + K - \alpha}{S + K + \alpha} \tag{15}$$

and S and K are the scattering and absorption coefficients, respectively.

The major advantage of this approach is that a simple closed form solution is obtained with only two constants: S and K. Unfortunately, the range of its validity and its theoretical basis are not well established and the two coefficients must be determined experimentally.

2 Materials and methods

The experimental determination of the relationship between optical density and cuvette depth for whole and haemolysed blood requires two separate systems: an extracorporeal blood circuit and a standard spectrophotometric arrangement.

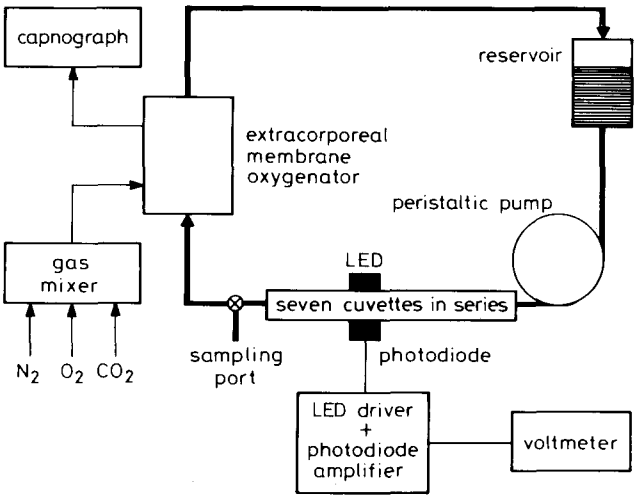

Fig. 1 *Blood circuit used in the in vitro experiments*

2.1 *In vitro blood circuit*

A closed-loop extracorporeal blood circuit is used to simulate gas exchange at the lungs, pulsatile blood flow and a vascular bed. The blood circuit is shown in Fig. 1. It comprises a reservoir, peristaltic pump, seven cuvettes and an extracorporeal membrane oxygenator. Such a system allows the oxygen saturation, pH and flow rate of the blood to be varied in a controlled manner.

2.2 *The cuvette*

The cuvettes are used to simulate blood flow through a vascular bed such as the fingertip or earlobe. The cuvettes essentially consist of a blood compartment sandwiched between two diffusers and thick layers of clear Perspex as shown in Fig. 2. Of course, this is a simplified model as no attempt is made to reproduce the anatomical network of capillaries, arterioles and venules.

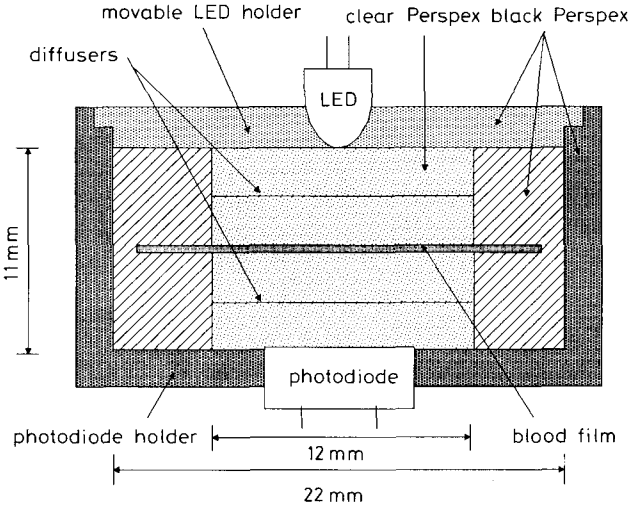

Fig. 2 *Cross-section of the cuvette and LED/photodiode arrangement used for optical density measurements*

To measure the optical density as a function of cuvette depth seven cuvettes were constructed with blood compartment depths of 0·20, 0·50, 0·75, 0·92, 1·15, 1·39 and 1·57 mm. The accurate measurement of cuvette depth was critical and hence the gaps, or depths, were measured after construction with feeler gauges. The relatively thick layers of Perspex around the blood film ensured that the depth of the blood film remained constant despite the pressure variations caused by the peristaltic pump. The blood inlets and outlets of the cuvettes were tapered to prevent flow separation.

The central 'window' of 12 mm diameter was made of clear Perspex and contained two diffusers made from translucent paper which had a very flat absorption spectrum in the wavelength range of interest. These diffusers were essential to simulate the optical properties of skin and other tissues. The penetration depth† in human tissue in the red to near-infra-red part of the spectrum has been found to be in the order of a few millimetres (WILSON and ADAM, 1983; ANDERSON and PARRISH, 1981). Hence, for a finger or earlobe of thickness 5–15 mm, the incident light gradually becomes diffuse as it penetrates the tissue and blood within it.

† *The depth at which collimated light becomes perfectly diffuse and is attenuated by 63 per cent according to photon diffusion theory.*

To investigate the effectiveness of the diffusers in our cuvettes, the intensity profile and angular distribution of the light incident on the blood film itself were measured (DE KOCK, 1991). The half-power diameters of the circular intensity profiles were found to be 2·5 and 4·5 mm for the red and infra-red LEDs, respectively. The half-power angles were found to be 29° and 38° for the red and infra-red LEDs, respectively. These figures showed that the diffusers were not ideal but they did provide spatial and angular averaging of the incident light which resulted in smoothing out of the variations in optical pathlengths in the blood film. However, the blood film itself is highly scattered at the haematocrits used, and the penetration depth of light in whole blood at the wavelengths employed in pulse oximetry is no more than 0·3–0·5 mm (TAKATANI *et al.*, 1980). Thus the combination of diffuser and blood film ensured that it was diffuse light which interacted with the bulk of the blood as *in vivo*. A diffuser was also located in front of the photodiode and thus increased its acceptance angle; hence the detected transmitted light would originate from a larger and more spatially averaged area.

The remainder of the cuvette was made of black Perspex to prevent stray light from interfering, and to eliminate light absorption by blood at the cuvette walls, where the blood flow may have been affected by boundary conditions.

2.3 *Pump*

The peristaltic pump (Marlow-Watson type MHRE881) produced a pulsatile blood flow to simulate cardiac output through the cuvette, membrane lung, and up to the reservoir. The pump generated sinusoidal output, at 70 cycles min^{-1}, to produce a mean flow rate of approximately 20 ml min^{-1}. A pump, rather than an elevated reservoir, was used because it was a better approximation to physiological conditions. Even with rigid cuvettes under these conditions, the transmitted light signal had a small pulsatile component (due to the changing orientations of the red blood cells). As we were interested in changes in light transmission due to volume changes (simulated here by cuvettes of different depths), the pulsatile component was filtered out.

2.4 *Extracorporeal membrane oxygenator*

An extracorporeal membrane oxygenator was used to control the oxygen saturation and pH of the blood. The membrane lung was composed of a single flat blood channel of 0·5 mm depth, sandwiched between two flat microporous isotactic polypropylene membranes (Celgard 2402) which were mounted against rigid support ribs on the gas side (DORRINGTON *et al.*, 1985). The device had an active area of $64 \times 160\,mm^2$ but a very small prime volume of only 5·1 ml.

A gas mixer was used to adjust the composition of the gas entering the membrane oxygenator by controlling the partial pressures of O_2, N_2 and CO_2 in the blood, the relative partial pressures of N_2 and O_2 determining the oxygen saturation. The partial pressure of CO_2 needed to be kept at approximately 5 kPa to maintain the blood pH at the right level. A capnograph (Gould Godhart Mark III) monitored the CO_2 content of the gas at the output of the membrane lung. The flow rate of CO_2 was adjusted to give a 5 per cent ($\pm$0·5 per cent) CO_2 content at all times. The gas was finally vented to the atmosphere.

The reservoir had a volume of 60 ml, with blood inlet at the top and outlet at the bottom. There were also gas inlets and outlets. The same gas as used by the membrane lung was also allowed to flow through the dead space above the blood in the reservoir. All the components of the blood circuit were connected together by PVC tubing (Portex, 4 mm inner diameter and 6 mm outer diameter).

2.5 *Optical system*

The optical density was measured using LEDs as light sources and a p-i-n photodiode as detector. The centre wavelengths of the LEDs were 660 nm (red, TLMP7005, Three-Five Systems Inc.) and 950 nm (infra-red, CQW13, TFK Inc.) and were typical of those used in pulse oximetry. A simple feedback circuit was used to provide a constant, but controllable, current to each LED. Once an LED had reached its operating temperature, the arrangement gave a light output which was very nearly constant. The LEDs were mounted in a separate holder which clamped onto the detector bracket at a predetermined position. In addition, each cuvette had location guides which allowed the LED/photodiode arrangement to be moved from cuvette to cuvette to allow for readings at the two wavelengths and for different depths on the same blood sample. The transmitted light intensity was detected by a p-i-n photodiode (Stanley PP210), and converted to a voltage using a standard transimpedance amplifier circuit.

2.6 *Experimental procedure*

Outdated whole human blood was obtained from the local Blood Transfusion Service. The blood was thoroughly mixed and filtered through a fine fabric mesh to remove aggregates and then centrifuged at 3000 rev min^{-1} for 20 min, to separate the red blood cells (RBCs) and plasma. The packed RBCs were resuspended in isotonic phosphate buffered saline (PBS) and recentrifuged. This washing procedure was repeated three times. After the final centrifugation, a 100 ml blood sample of 15·8 g dl^{-1} haemoglobin concentration (as measured by a Radiometer OSM-3 Hemoximeter) was made up by mixing appropriate amounts of packed red blood cells and PBS. The haematocrit level of the blood sample was found to be 50 ± 2 per cent as measured by the microcapillary method. The concentrations of carboxyhaemoglobin and methaemoglobin were always found to be less than 1 per cent as measured by the Hemoximeter, and hence would not have caused any significant error.

The following experiment was performed to measure the relationship between optical density and cuvette depth for whole blood over a wide range of oxygen saturations. The blood sample was introduced into the blood circuit, and a mixture of 95 per cent oxygen and 5 per cent CO_2 was allowed to flow through the membrane lung and reservoir. The system was then given time to saturate fully and equilibrate to room temperature. The oxygen saturation SaO_2 was verified to be 98–100 per cent by the Hemoximeter. At this point, the transmitted light intensity I for each of the seven cuvettes was recorded at both wavelengths. To desaturate the blood, the oxygen passing through the membrane lung was replaced by a mixture of 95 per cent N_2 and 5 per cent CO_2.

As the saturation slowly reduced over a period of 3 h, the light intensity readings, as described above, were taken at intervals corresponding to changes in SaO_2 of approximately 10 per cent. The saturation levels were measured just before and just after the light intensity readings using the Hemoximeter, and remained constant to within 3 per cent of the initial measurement (this variation being caused by having to take measurements on seven cuvettes in turn).

With the use of an N_2 and CO_2 gas mixture, it was very difficult to desaturate the blood fully; to obtain readings at 0 per cent saturation, a small quantity of a chemical reduction agent, sodium hydrosulphite ($Na_2S_2O_4$), was added until the oxygen saturation dropped to less than 0·5 per cent SaO_2 (as measured by the Hemoximeter). Finally, the blood was removed from the system by flushing and rinsing with water. After replacing the water with PBS, the value of I_0 was recorded for each cuvette at both wavelengths.

The above experiment was also repeated with haemoglobin solutions. The latter were prepared by washing whole blood samples in PBS as described previously and then haemolysing them by ultrasound disruption. The red blood cell ghosts were precipitated by ultracentrifugation for 30 min at 32 000 rev min^{-1}. Haemolysis was verified by microscopic examination. Readings were only taken for fully oxygenated and fully deoxygenated haemoglobin solutions at the concentration of 15·8 g dl^{-1}, as only the Hb and HbO_2 extinction coefficients were required for the theoretical model based on the Beer-Lambert law relating SaO_2 and the R:IR ratio.

From the data gathered with this set of experiments, it was possible to obtain plots of optical density against cuvette depth for whole blood over the entire saturation range at approximately 10 per cent SaO_2 intervals and for Hb and HbO_2 solutions at wavelengths of 660 and 950 nm.

3 Results and analysis

The experimental results obtained with the haemoglobin solutions allowed the millimolar extinction coefficients of Hb and HbO_2 to be calculated for our optical arrangement. These extinction coefficients were required both for the theoretical model for haemolysed blood and the analysis of whole blood data (Twersky's theory, eqn. 9). The graphs of optical density against cuvette depth for Hb and HbO_2 solutions at both 660 and 950 nm at a haemoglobin concentration of 15·8 g dl^{-1} are shown in Fig. 3. To determine the extinction coefficients, the Beer-Lambert law was fitted to the experimental data using a least-squares criterion. The best-fit regression lines are also shown in Fig. 3, and the values of the extinction coefficients obtained from these data are summarised in Table 1. It should be noted that the values are particular to our cuvettes (with diffusers) and LEDs (with finite bandwidths). However, they are in general agreement with the monochromatic extinction coefficients published by VAN ASSENDELFT (1970) and MENDELSON and KENT (1989) also listed in Table 1.

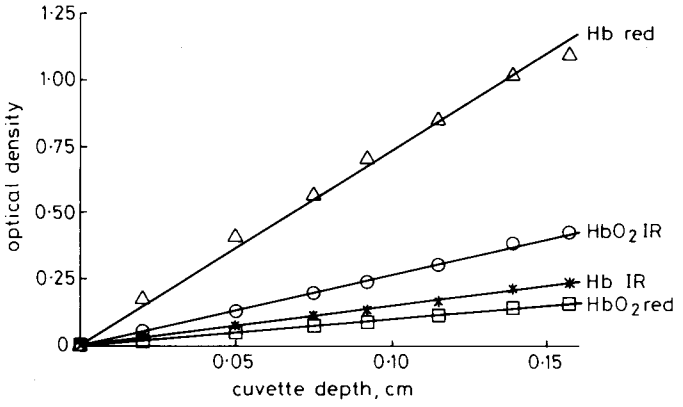

Fig. 3 *Optical density of Hb and HbO_2 solutions as a function of cuvette depth for both red and infra-red wavelengths*

The analysis of the experimental data from RBC suspensions is more complicated as we are investigating three different theoretical models, all of which are nonlinear and include parameters which have to be determined empirically by curve fitting: S and K with the Kubelka-Munk theory, S_0 and ε with photon diffusion theory, and finally a, q and q' with Twersky's theory. This was performed for all three models, for oxygenated and deoxygenated RBC suspensions and for both wavelengths, by running a statistical analysis system (SAS) software package on a VAX 8800 computer. The values of the constants which gave the best fit to our data are summarised in Table 2.

Our values for the constants are not in close agreement with those published. Our values of a and q in Twersky's theory, for example, are approximately out by a factor of 2 and 0·3, respectively, when compared with the values obtained by STEINKE and SHEPHERD (1986). Our values for the constants ε and S_0 used in the photon diffusion model are also significantly greater than those found by Steinke and Shepherd. These discrepancies, however, are not surprising as there are major differences between their experimental setup and ours.

First, Steinke and Shepherd, as others in the literature, obtained the constants by curve fitting on optical density data as a function of haematocrit instead of cuvette depth. Secondly, the blood flow in our cuvettes was pulsatile compared with steady flow under gravity (STEINKE and SHEPHERD, 1986) or measurements on static blood (LOEWINGER *et al.*, 1964; ANDERSON and SEKELJ, 1967). Thirdly, the optical arrangement is also an important factor; q and q' in Twersky's theory both depend on the

Table 1 Hb and HbO_2 extinction coefficients in litre $mmol^{-1}$ cm^{-1} as determined by optical density measurements from cuvettes of varying depths

Wavelength, nm	Hb	HbO_2	Hb*	HbO_2*	Hb†	HbO_2†
660	0·747	0·102	0·80	0·08	0·86	0.12
950	0·154	0·272	0·20	0·30	0·20	0·29

*Data from VAN ASSENDELFT (1970).
†Data from MENDELSON and KENT (1989).

Table 2 Best fit values of constants for Twersky's, Kubelka-Munk and photon diffusion theories to the optical density measurements of both oxygenated and reduced whole blood

		Twersky				Kubelka-Munk			Photon diffusion		
	Wavelength, nm	a	q	q'	RMS error per cent	S	K	RMS error per cent	ε	S_0	RMS error per cent
HbO_2	660	50·14	0·240	1·00	4·33	37·82	1·05	1·52	0·710	0·145	12·7
	950	42·12	0·138	1·00	2·26	27·18	7·20	0·97	0·149	0·044	1·1
Hb	660	87·99	0·247	0·505	1·8	111·32	4·26	2·57	1·322	0·015	11·2
	950	44·93	0·280	1·00	2·74	30·08	2·75	1·13	0·776	0·126	8·6

photodetector aperture angle and the position and size of the emitter/detector arrangement.

Our cuvettes diffused the light before and after interaction with the blood film (see Section 2.2). The nature of the incident light is important as diffuse and collimated light are not absorbed and scattered in the same way: for example JANSSEN (1972) showed that the extinction coefficient for perfectly diffuse light is double that of collimated light. ANDERSON and SEKELJ (1965) found that their measurements of the optical properties of whole blood using diffuse illumination were significantly different than those obtained by KRAMER *et al.* (1951), who used collimated

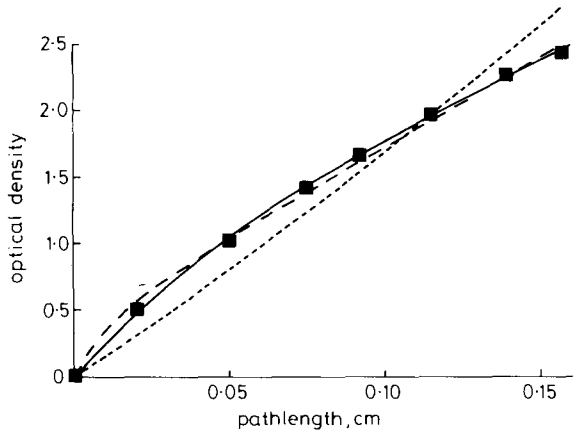

Fig. 4 *The best fit of Twersky's (solid line, RMS error = 1·8 per cent), Kubelka-Munk (broken line, RMS error = 2·6 per cent), and photon diffusion theories (dotted line, RMS error = 11·1 per cent), to the optical density data of reduced whole blood at 660 nm*

light. Anderson and Sekelj considered the difference to be due to the type of illumination.

To the best knowledge of the authors, no data for Twersky's theory have been reported for measurements on pulsatile flowing whole blood using diffused light.

Fig. 4 shows the result of fitting Twersky's, photon diffusion and Kubelka-Munk theories to the optical density data of deoxygenated blood at 660 nm wavelength. These graphs are typical of the results obtained at other wavelengths and saturations.

The RMS errors between the best-fit curves and the data showed that the Twersky and Kubelka-Munk models gave a better fit (RMS error of 1·8 and 2·6 per cent, respectively) to our results than Zdrojkowski and Pisharoty's photon diffusion approach (RMS error = 11·1 per cent). Twersky's theory has previously been shown to model the optical properties of whole blood as a function of haematocrit with a high degree of accuracy (STEINKE and SHEPHERD, 1986) and was therefore selected for all further analysis.

4 Pulse oximetry models

4.1 *R:IR ratio for haemoglobin solutions*

Consider a cuvette of depth D containing a mixture of HbO_2 and Hb solutions, which has a small degree of flexibility and thus expands by ΔD if the driving pressure is increased. This is a first-order model of an artery. Fig. 5 shows how a flexible cuvette can be modelled by two rigid cuvettes, one of depth D and the other of depth $D + \Delta D$. The total light transmitted through a cuvette depth of $D + \Delta D$, at red and infra-red wavelengths, is as follows, according to the Beer-Lambert Law:

$$I_{total1} = I_{(DC+AC)_1} = I_0\, 10^{-(\varepsilon_{o1}C_o + \varepsilon_{r1}C_r)D} 10^{-(\varepsilon_{o1}C_o + \varepsilon_{r1}C_r)\Delta D} \tag{16}$$

$$I_{total2} = I_{(DC+AC)_2} = I_0 10^{-(\varepsilon_{o2}C_0 + \varepsilon_{r2}C_r)D} 10^{-(\varepsilon_{o2}C_o + \varepsilon_{r2}C_r)\Delta D} \tag{17}$$

where ε_o and ε_r are the extinction coefficients of HbO_2 and Hb, respectively, and the numerical subscripts 1 and 2 refer to the red (λ_1) and IR (λ_2) wavelengths, respectively. If we divide both sides by I_{DC} (i.e. $I_0\, 10^{(\varepsilon_o C_o + \varepsilon_r C_r)D}$) and rearrange, we can obtain the R:IR ratio which we have defined in a similar way to YOSHIYA *et al.* (1980):

$$\frac{R}{IR} = \frac{\log\,(I_{(DC+AC)1}/I_{DC1})}{\log\,(I_{DC+AC)2}/I_{DC2})} = \frac{\varepsilon_{o1}C_o + \varepsilon_{r1}C_r}{\varepsilon_{o2}C_o + \varepsilon_{r2}C_r} \tag{18}$$

Eqns. 1 and 18 can then be combined to give a theoretical expression for the oxygen saturation of Hb solutions.

$$SaO_2 = \frac{\varepsilon_{r2}\dfrac{R}{IR} - \varepsilon_{r1}}{(\varepsilon_{r2} - \varepsilon_{o2})\dfrac{R}{IR} - (\varepsilon_{r1} - \varepsilon_{o1})} \tag{19}$$

Note that this equation has no concentration or depth dependence.

Using the extinction coefficients ε for haemoglobin solutions from Table 1 and substituting them into eqn. 19 gives an SaO_2 of 100 per cent when R:IR = 0·30 and an SaO_2 of 0 per cent when R:IR = 4·85. Thus by varying the R:IR ratio from 0·30 to 4·85 we can construct a theoretical

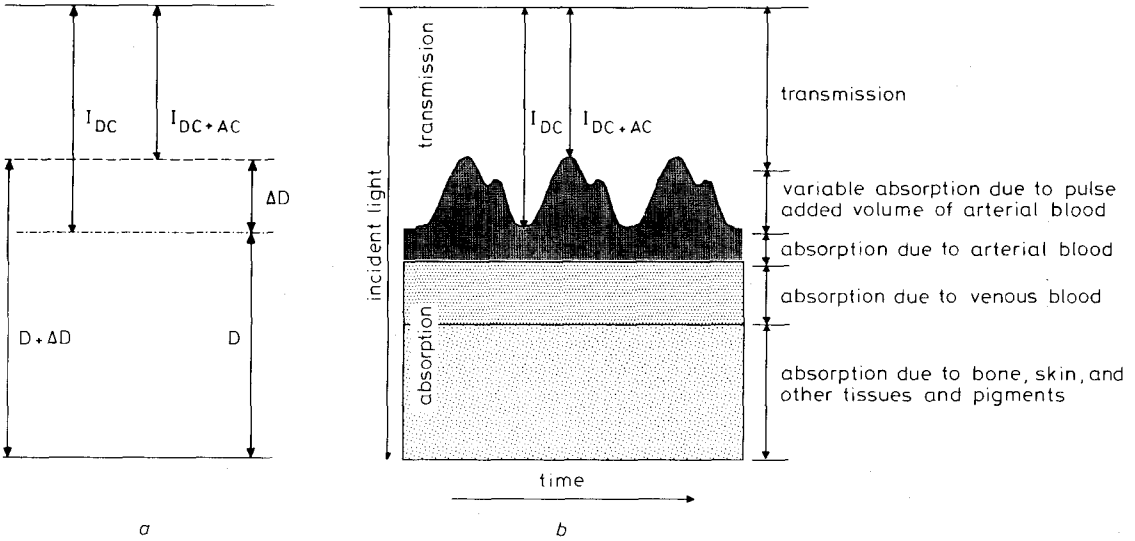

Fig. 5 *Comparison between cuvette model and the light transmission in a vascular bed*

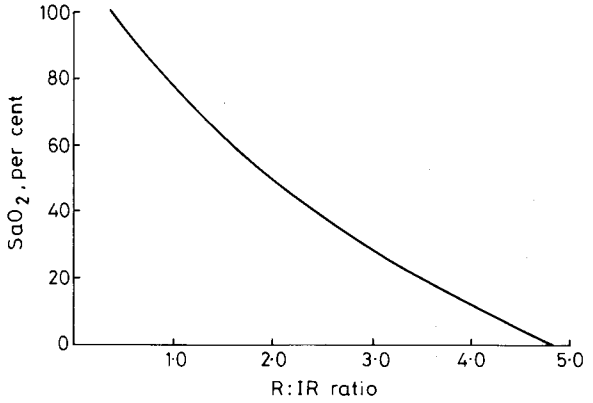

Fig. 6 *Theoretical relationship between SaO_2 and the R:IR ratio for haemoglobin solutions, as predicted by a simple model based on the Beer-Lambert Law. See text for a definition of the R:IR ratio*

graph for the variation of the SaO_2 with R:IR ratio (the convention in pulse oximetry is to plot this relationship with the axes as shown in Fig. 6).

4.2 *R:IR ratio for whole blood*

4.2.1 *As a function of depth.* The analysis for whole blood required a different approach because of the nonlinear relationship between optical density and cuvette depth. Let the transmitted light intensity I be a nonlinear function $f(x)$, where x is the cuvette depth.

$$I = I_0 f(x) \tag{20}$$

where $f(x) = 10^{OD(x)}$ and $OD(x)$, the optical density as a function of depth, was assumed to have been determined by fitting Twersky's equation to the experimental data (as in Fig. 4). We then constructed a plot of $f(x)$ as a function of depth for our cuvettes, and this is shown, for the red wavelength, in Fig. 7. To compute the R:IR ratio for whole blood we needed to determine the quantity log (I_{DC+AC}/I_{DC}) at both wavelengths. Using the model of Fig. 5, as before, we considered I_{DC+AC} to be equivalent to $I_0 f(D + \Delta D)$, and I_{DC} to $I_0 f(D)$, and wrote:

$$\frac{I_{(DC+AC)1}}{I_{DC1}} = \frac{f_1(D + \Delta D)}{f_1(D)} \tag{21}$$

$$\frac{I_{(DC+AC)2}}{I_{DC2}} = \frac{f_2(D + \Delta D)}{f_2(D)} \tag{22}$$

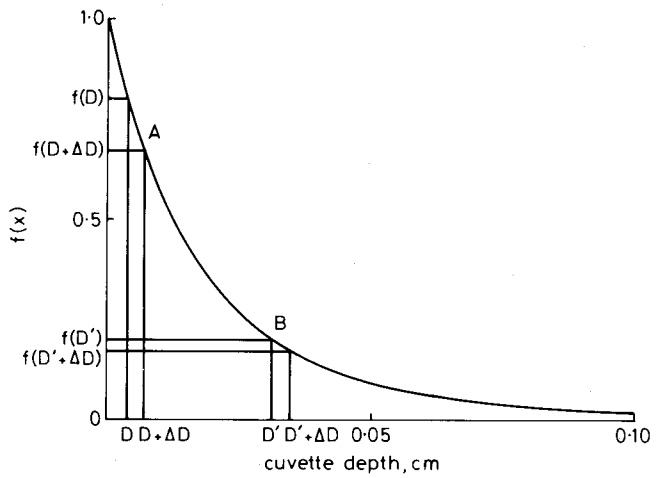

Fig. 7 *Relationship between $f(x)$ and cuvette depth for blood with a saturation of 0 per cent at the red wavelength. The derivation of the $f(D)$ and $f(D + \Delta D)$ terms is also shown for two different values of x (D and D')*

The R:IR ratio is now given by:

$$\frac{R}{IR} = \frac{\log\left[\dfrac{f_1(D + \Delta D)}{f_1(D)}\right]}{\log\left[\dfrac{f_2(D + \Delta D)}{f_2(D)}\right]} \tag{23}$$

The major difference between the R:IR ratio for whole blood and the R:IR ratio for haemoglobin solutions is the former's dependence on cuvette depth. At either wavelength, λ_1 or λ_2, the ratio $f(D + \Delta D)/f(D)$ varies with the value of D (see points A and B on Fig. 7), whereas, of course, it does not for haemoglobin solutions because optical density is a linear function of depth.

In clinical practice, however, pulse oximeters have been found to give accurate results with tissue beds which have a wide range of blood content and arterial pulsations. This would indicate that pulse oximeter readings are unaffected by the actual pathlength over which the measurements are made. Our hypothesis, therefore, is that the nonlinear dependence of $f(x)$ is, to all intents and purposes, independent of wavelength over the wavelength range λ_1–λ_2. To investigate this, we computed the value of I_{DC+AC}/I_{DC} for gradually increasing values for D, for both the red and infra-red wavelengths for whole blood. The results for blood with an oxygen saturation of 0 per cent are shown in Fig. 8*a* (note the compressed scale on the vertical axis). It is clear that the ratios $f_1(D + \Delta D)/f_1(D)$ and $f_2(D + \Delta D)/f_2(D)$, when plotted as a function of cuvette depth, show similar trends (see Figs. 8*a* and 8*b* for blood at 0 and 100 per cent saturation, respectively). When we take the logarithms of $f(D + \Delta D)/f(D)$ at both wavelengths and derive from these the R:IR ratio for different depths, we obtain an approximately straight horizontal line for blood at both 100 and 0 per cent saturation (Fig. 9). The depen-

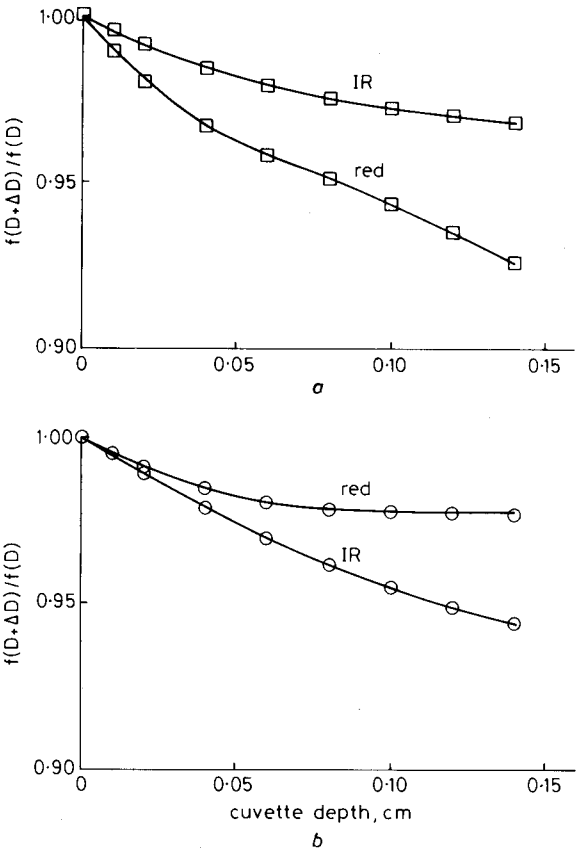

Fig. 8 *The variation of the ratio $[f(D + \Delta D)/f(D)]$ as a function of cuvette depth for both the red and IR wavelengths. Data are shown for oxygen saturations of 0 and 100 per cent in Fig. 11, respectively. The 'pulsatility' ΔD is 2 per cent*

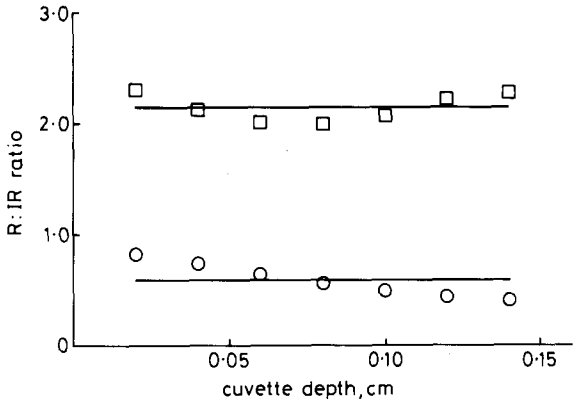

Fig. 9 *R:IR ratio plotted as a function of cuvette depth for blood with a saturation of 0 per cent (□) and 100 per cent (○)*

dence on cuvette depth is largely cancelled out in the R:IR ratio and hence a pulse oximeter monitoring this ratio will not be unduly affected by variations in optical pathlength.

4.2.2 *As a function of* SaO_2. If the R:IR ratio is to be used to measure oxygen saturation in whole blood, then it is necessary to have explicit knowledge of $f(x)$ at all saturations. From our measurements at approximately every 10 per cent SaO_2, we computed the values of the constants in Twersky's theory at these intermediate saturations for both wavelengths. Fig. 10 shows the best fit curves using Twersky's theory for optical density measurements at selected saturations for the red (660 nm) wavelength. Note the nonlinearity of the optical density as a function of saturation.

Thus an estimate of $f(x)$ for all cuvette depths, over a range of saturations, at both red and IR wavelengths, was obtained. The ratio $f(D + \Delta D)/f(D)$ could again be constructed from the curve of $f(x)$, and eqn. 23 could be used to compute the R:IR ratio at all the values of SaO_2 for which measurements were taken (approximately every 10 per cent SaO_2). The result is shown in Fig. 11. Each point on the graph corresponds to the mean value of the R:IR ratios computed for depths D of 0·2, 0·4, 0·6, 0·8, 1·0, 1·2 and 1·4 mm. The 'pulsatility' ΔD was chosen in all cases to be 2 per cent of the depth D. Varying the degree of 'pulsatility' ΔD from 1 to 5 per cent had virtually no effect (less than 1 per cent error) on the results over the whole saturation range.

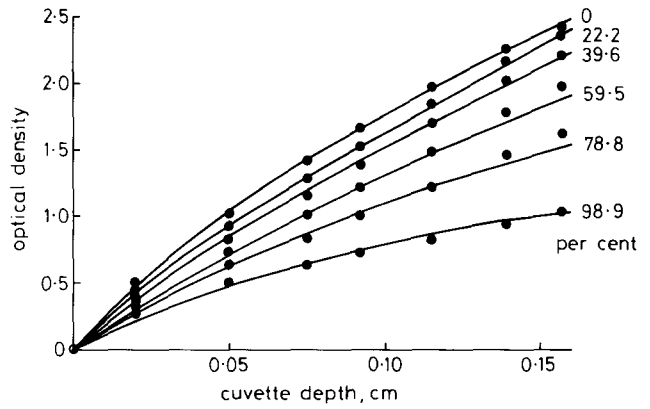

Fig. 10 *Best fit curves of Twersky's theory to the optical density measurements of reduced whole blood as a function of cuvette depth at selected oxygen saturations. Data shown correspond to measurements taken at the red (660 nm) wavelength*

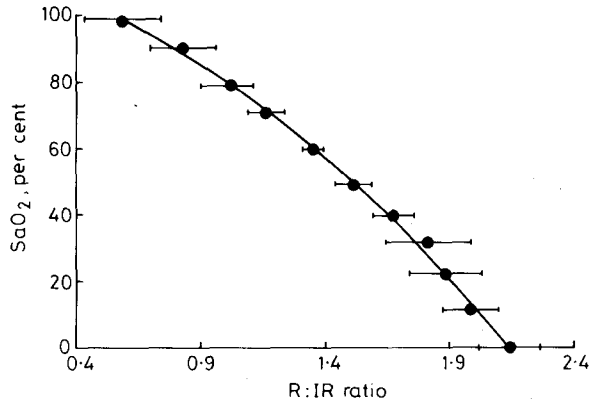

Fig. 11 *Relationship between SaO_2 and the R:IR ratio as predicted by our model based on the optical properties of whole blood as described by Twersky's theory. Each point corresponds to the mean of the R:IR ratios calculated at depths (D) of 0·2, 0·4, 0·6, 0·8, 1·0, 1·2 and 1·4 mm, and the error bars represent the standard deviation. The 'pulsatility' (ΔD) was 2 per cent of the cuvette depth D*

5 Validation of theoretical model

To validate our theoretical model, we used the results from our previous paper (DE KOCK and TARASSENKO, 1991) in which we made measurements of the R:IR ratio at different values of SaO_2 using similar instrumentation but with flexible cuvettes. In this case the transmitted light intensity readings corresponding to both I_{DC} and I_{DC+AC}

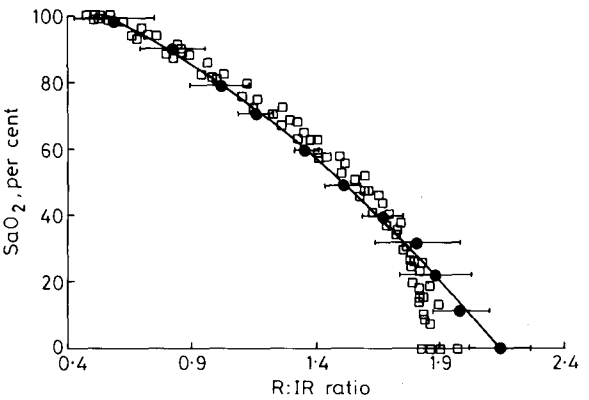

Fig. 12 *Comparison of results predicted by our model (Fig. 11), and our previous entirely empirical measurements taken from flexible cuvettes (DE KOCK and TARASSENKO, 1991)*

could be measured directly at the appropriate point in the pressure cycle. The SaO_2 was plotted against the value of the R:IR ratio, computed from the I_{DC} and I_{DC+AC} measurements at both wavelengths (see eqn. 18) and the results obtained from our experiments (with similar haematocrits, flow rates and a cuvette depth of 1 mm) are shown in Fig. 12. We have also included in this figure the curve predicted by our theoretical model. It can clearly be seen that the direct experimental results obtained from the flexible cuvette are in very good agreement with the predictions of the theoretical model, which gives both the position and convex shape of the curve.

The final question to be answered concerns the validity of the flexible cuvette as an *in vitro* model to simulate the vascular bed. To answer that question, a final experiment was conducted whereby a commercial instrument (the Nellcor N100, which like all other pulse oximeters is calibrated from *in vivo* data) was attached to the flexible cuvette, as if it were a finger, and the SpO_2 and SaO_2 values were simultaneously recorded as the oxygen saturation of the blood in the extracorporeal blood circuit was gradually reduced.

The results of two of these experiments are plotted in Fig. 13, and it is immediately evident that the SpO_2 values recorded from the cuvette lie close to the line of identity from 100 to 30 per cent SaO_2 (below this saturation the optical density for the red wavelength was too high for the pulse oximeter to continue to give readings). However, the pulse oximeter consistently overestimated the oxygen saturation by 4·1 per cent (SD = 1·1 per cent).

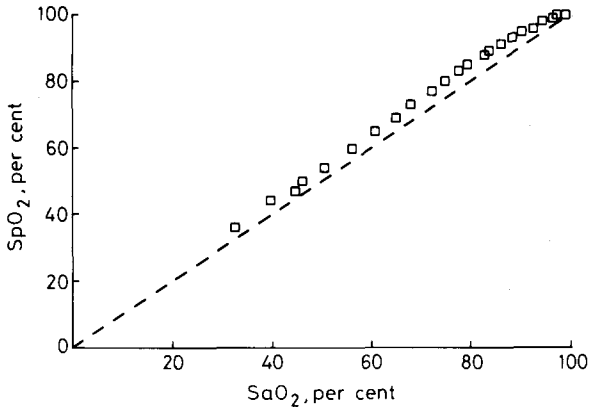

Fig. 13 *In vitro relationship between SpO_2 readings from a Nellcor N100 pulse oximeter and SaO_2 measurements from a blood sample obtained by using a flexible cuvette. The data are from two experiments, and the broken line represents identity*

This small overestimation could be due to the fact that our cuvettes did not model the anatomical network of arterioles, capillaries and venules, nor the presence of venous blood. In addition, our diffusers were only a simple analogue of the optical absorption and scattering properties of the skin and tissues. Nevertheless, the agreement between the SpO_2 values from the instrument and the SaO_2 values from the whole blood is surprisingly good considering the simplicity of the *in vitro* model.

6 Conclusion

In this paper we have repeated the work of STEINKE and SHEPHERD (1986), who investigated theoretical models of the optical properties of whole blood. In our work, however, we modelled these properties as a function of depth rather than haematocrit using pulsatile blood flow generated by the peristaltic pump. Like Steinke and Shepherd, we found that Twersky's theory gave a good fit to our experimental data not only for wholly saturated or desaturated blood but also for intermediate values of SaO_2 (Fig. 10). We used the best-fit curves of optical density as a function of cuvette depth to predict the value of the R:IR ratio, as used in pulse oximetry, for varying SaO_2.

The simple theoretical model which we used to derive the R:IR ratio (eqn. 23) takes into account the nonlinear relationship between optical density and cuvette depth. However, we showed clearly that the R:IR ratio does not overly depend (SD = 0·14 at 100 per cent SaO_2) on cuvette depth because the ratio involves the measurement of the optical properties at two wavelengths close enough (in relation to the size of the red blood cells) for scattering effects to be similar. Hence our graph of SaO_2 against the R:IR ratio is an average of all our measurements for seven different depths (albeit at constant 'pulsatility').

To validate the prediction of our theoretical model, we used results of a previous experiment in which the relationship between SaO_2 and the R:IR ratio was recorded from a flexible cuvette (DE KOCK and TARASSENKO, 1991). These experimental values were found to lie within one standard deviation of the curve predicted by our theoretical model. Finally, the validity of using a flexible cuvette as a model of a vascular bed was also confirmed experimentally by measuring the relationship between SpO_2 values from a commercial pulse oximeter and SaO_2 for whole blood.

We would argue that the last two results are important developments in the understanding and evaluation of the technique of pulse oximetry:

(*a*) We now have, for the first time, a reasonably accurate model of the relationship between SaO_2 and the R:IR ratio based on whole blood not haemoglobin solutions.
(*b*) The type of flexible cuvette used in our work is a valid model of a vascular bed which could be used for calibration studies on commercial pulse oximeters.

References

ANDERSON, N. M. and SEKELJ, P. (1965) Studies on the light transmission of non-hemolysed whole blood. Determination of oxygen saturation. *J. Lab. & Clin. Med.*, **63,** 153–166.

ANDERSON, N. M. and SEKELJ, P. (1967) Light absorbing and scattering properties of non-haemolysed blood. *Phys. in Med. & Biol.*, **12,** 173–184.

ANDERSON, R. R. and PARRISH, J. A. (1981) The optics of human skin. *J. Invest. Dermatol.*, **77,** 13–19.

DE KOCK, J. P. (1991) Pulse oximetry: theoretical and experimental models. D. Phil. Thesis, University of Oxford.

DE KOCK, J. P. and TARASSENKO, L. (1991) *In vitro* investigation of the factors affecting pulse oximetry. *J. Biomed. Eng.*, **13,** 61–66.

DORRINGTON, K. L., RALPH, M. E., BELLHOUSE, B. J., GARDAZ, J.-P. and SYKES, M. K. (1985) Oxygen and CO_2 transfer of a polypropylene dimpled membrane lung with variable secondary flows. *Ibid.*, **7,** 89–99.

ISHIMARU, A. (1978) *Wave propagation and scattering in random media*, vol. 1. Academic Press.

JANSSEN, F. J. (1972) A study of the absorption and scattering factors of light in whole blood. *Med. & Biol. Eng.*, **10,** 231–240.

JOHNSON, C. C. (1970) Near infrared propagation in blood. *J. Assoc. Adv. Med. Instrm.*, **4,** 22–27.

KRAMER, K., ELAM, J. O., SAXTON, G. A. and ELAM, W. N. (1951) Influence of oxygen saturation, erythrocyte concentration and optical depth upon the red and near-infrared light transmittance of blood. *Am. J. Physiol.*, **165,** 229–246.

KUBELKA, P. and MUNK, F. (1931) Ein Betrag zur Optik der Farbanstriche. *Z. Techn. Phys.*, **12,** 593–601.

LIPOWSKY, S., USAMI, S., CHIEN, S. and PITTMAN, R. N. (1980) Haematocrit determination in small bore tubes from optical density measurements under white light illumination. *Microvasc. Res.*, **20,** 51–70.

LOEWINGER, E., GORDON, A., WEINREB, A. and GROSS, J. (1964) Analysis of a micromethod for transmission oximetry of whole blood. *J. Appl. Physiol.*, **19,** 1179–1184.

MENDELSON, Y. and KENT, J. C. (1989) Variations in optical absorption spectra of adult and fetal haemoglobins and its effect on pulse oximetry. *IEEE Trans.*, **BME-36,** 844–848.

PAYNE, J. P. and SEVERINGHAUS, J. W. (Eds.) (1986) *Pulse oximetry*. Springer Verlag, New York.

SEVERINGHAUS, J. W. and NAIFEH, K. H. (1987) Accuracy of response of six pulse oximeters to profound hypoxia. *Anesthesiol.*, **67,** 551–558.

SHIMADA, Y., YOSHIYA, I., OKA, N. and HAMAGURI, K. (1984) Effects of multiple scattering and peripheral circulation on arterial oxygen saturation measured with a pulse-type oximeter. *Med. & Biol. Eng. & Comput.*, **22,** 475–478.

SHOCKLEY, W. (1962) Diffusion and drift of minority carriers in semiconductors for comparable capture and scattering mean free paths. *Phys. Rev.*, **125,** 1570–1576.

STEINKE, J. M. and SHEPHERD, A. P. (1986) Role of light scattering in whole blood oximetry. *IEEE Trans.*, **BME-33,** 294–301.

TAKATANI, S., CHEUNG, P. W. and ERNST, E. A. (1980) A nonin-

vasive tissue reflectance oximeter—an instrument for measurement of tissue hemoglobin oxygen saturation *in vivo*. *Ann. Biomed. Eng.*, **8,** 1–15.
TWERSKY, V. (1962) Multiple scattering of waves and optical phenomena. *J. Opt. Soc. Am.*, **52,** 145–171.
TWERSKY, V. (1970*a*) Interface effects in multiple scattering by large, low refracting absorbing particles. *Ibid.*, **60,** 908–914.
TWERSKY, V. (1970*b*) Absorption and multiple scattering by biological suspensions. *Ibid.*, **60,** 1084–1093.
VAN ASSENDELFT, O. W. (1970) *Spectrophotometry of haemoglobin and its derivatives.* Royal Vangorcum Ltd., Assen, The Netherlands.
WILSON, B. C. and ADAM, G. (1983) A Monte Carlo model for the absorption and flux distribution of light in tissue. *Med. Phys.*, **10,** 824–830.
WUKITSCH, M. W., PETTERSON, N. T., TOBLER, D. R. and POLOGE, J. A. (1988) Pulse oximetry: analysis of theory, technology, and practice. *J. Clin. Monit.*, **4,** 290–301.
YOSHIYA, I., SHIMADA, Y. and TANAKA, K. (1980) Spectrophotometric monitoring of arterial oxygen saturation in the fingertip. *Med. & Biol. Eng. & Comput.*, **18,** 27–32.
ZDROJKOWSKI, R. J. and PISHAROTY, N. R. (1970) Optical transmission and reflection of blood. *IEEE Trans.*, **BME-17,** 122–128.

Authors' biographies

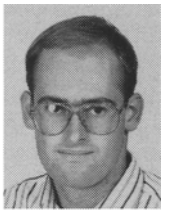

Joost P. de Kock is a doctoral research student in the Medical Engineering Unit, Department of Engineering Science, University of Oxford, UK. He graduated with a first class BA degree in Electrical & Information Sciences from Cambridge University, UK, in 1988. His research interests include non-invasive optical measurements of blood oxygen saturation and haematocrit.

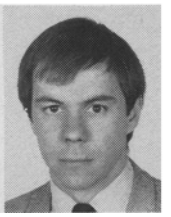

After graduating from the University of Oxford, UK, with a degree in Engineering Science, Lionel Tarassenko worked in an industrial research laboratory on the development of new digital signal processing techniques. He then returned to the University of Oxford to undertake research in medical electronics and physiology. Since being appointed a University Lecturer in 1988, he has continued to work on the applications of electronics to medicine but his main research interest has been the investigation of artificial neural networks and their application to a wide range of problems.